

Heavy-element abundances in the CH/CN-strong very metal-poor stars CS 22948-27 and CS 29497-34*

V. Hill^{1,2}, B. Barbuy³, M. Spite², F. Spite², R. Cayrel⁴, B. Plez⁵, T.C. Beers⁶, B. Nordström⁷, and P.E. Nissen⁸

¹ European Southern Observatory, Karl-Schwarzschild-Strasse 2, 85748 Garching bei München, Germany (vhill@eso.org)

² Observatoire de Paris-Meudon, DASGAL, URM 8633 du CNRS, 92195 Meudon Cedex, France (Monique.Spite, Francois.Spite@obspm.fr)

³ Universidade de São Paulo, CP 3386, São Paulo 01060-970, Brazil (barbuy@orion.iagusp.usp.br)

⁴ Observatoire de Paris, DASGAL, URM 8633 du CNRS, 61 Av. de l'Observatoire, 75014 Paris, France (Roger.Cayrel@obspm.fr)

⁵ GRAAL cc72, Université de Montpellier II, 34095 Montpellier Cedex 5, France (plez@graal.univ-montp2.fr)

⁶ Michigan State University, Department of Physics and Astronomy, East Lansing, MI 48824, USA (beers@pa.msu.edu)

⁷ Niels Bohr Institute for Astronomy, Physics and Geophysics, Copenhagen University, Juliane Maries Vej 30, 2100 Copenhagen, Denmark (birgitta@astro.ku.dk)

⁸ Institute of Physics and Astronomy, Aarhus University, 8000 Aarhus C, Denmark (pen@obs.aau.dk)

Received 26 July 1999 / Accepted 2 November 1999

Abstract. We have carried out a new analysis of the very metal-poor CH/CN strong stars CS 22948-27 and CS 29497-34. In particular, the effective temperatures were recomputed by comparing newly obtained photometric data to colours derived from model atmospheres computed especially for these stars. Metallicities of $[Fe/H] = -2.45$ and -2.90 are found, respectively, for CS 22948-27 and CS 29497-34.

The abundances of heavy elements have been derived from newly obtained high-resolution spectroscopy in the blue spectral region, together with previously obtained spectra in the red, resulting in a total wavelength coverage of $\lambda\lambda$ 4000–8200 Å.

We find that the abundance patterns of our stars reflect enrichment by the *r*-process (as indicated by a high Eu abundance), as well as by the *s*-process, which could be due to a mass transfer episode from a companion crossing the AGB phase, although no clear evidence for binarity is indicated in the spectra obtained to date.

Key words: stars: abundances – stars: fundamental parameters – stars: general

1. Introduction

The Beers et al. (1985, 1992) HK interference-filter/ objective-prism survey of very metal-poor stars has identified an unexpected number of carbon-rich and often also nitrogen-rich stars in the metallicity range $-3.5 < [Fe/H] < -2.5$ (see for example Rossi et al. 1999). These stars are often (but not in every case) also enriched in neutron-capture *s* elements, suggesting an intrinsic post-AGB enrichment in the star, or mass transfer in a binary system in which one component is a former Asymp-

totic Giant Branch (AGB) star (McClure et al. 1980, McClure & Woodsworth 1990).

We have obtained high-resolution spectra for two such stars discovered in the HK survey, CS 22948-27 and CS 29497-34, at coordinates $(l, b) = (3.05^\circ, -48.23^\circ)$ and $(52.81^\circ, -87.67^\circ)$, $J2000 (\alpha, \delta) = (21^h 37^m 45.5^s, -39^\circ 27' 19'')$ and $(00^h 41^m 39.9^s, -26^\circ 18' 55'')$, respectively. A preliminary analysis of the elemental abundances of these stars was given in Barbuy et al. (1997, hereafter Paper I).

In this paper we carry out a new analysis for these two stars, with the following main improvements relative to Paper I: **(a)** the spectral range of our high-resolution spectra was enlarged, in order to include the blue part of the spectrum as well as the red region. For many neutron-capture elements the most suitable lines for detailed abundance analysis lie in the blue. This has allowed us to increase the number of measurable neutron-capture elements to nine; **(b)** a new derivation of effective temperatures based on *BVRI* photometry obtained at the ESO 0.9 Dutch telescope was carried out, **(c)** a new grid of atmospheric models was used, with chemical compositions closer to the approximate elemental abundances for these stars, which are quite different from other non C- and N- enriched stars. New opacities and new models were computed for these peculiar chemical compositions, which have significant weight in molecular-line absorption due to C₂, CH and CN bands. **(d)** new high-resolution spectra were obtained in 1999 in order to check for possible radial velocity variations.

Finally, a new and important piece of information has been added. These two stars have measured proper motions from two independent sources. Both obtain a significant proper motion, excluding the possibility that these stars are distant, and thus very luminous.

In Sect. 2 the observations and reduction procedures are reported. In Sect. 3 the spectrum synthesis calculations and abundance determinations are described. In Sect. 4 the results are

Send offprint requests to: B. Barbuy

* Observations collected at the European Southern Observatory (ESO), La Silla, Chile.

Table 1. Log of the observations.

Star	date	exp. (min)	λ (Å)	S/N	V_{rHeI} km s^{-1}
CASPEC					
CS 22948-27	01-10-96	90	4000-5000	110	-60.6
	02-10-96	120	4000-5000	150	-67.3
CS 22497-34	01-10-96	120	4000-5000	170	-43.3
	02-10-96	120	4000-5000	190	-42.2
EMMI					
CS 22948-27	15-09-95	120	5000-8200	170	-63.9
	17-09-95	105	5000-8200	180	-64.7
	03-11-95	60	5000-8200	58	-62.3
	04-11-95	60	5000-8200	56	-62.7
	05-11-95	55	5000-8200	53	-62.8
CS 22497-34	14-09-95	120	5000-8200	220	-44.6
	14-09-95	95	5000-8200	175	-44.7
	03-11-95	90	5000-8200	90	-46.6
	04-11-95	75	5000-8200	76	-45.7
FEROS					
CS 22948-27	15-07-99	30	4000-8500	30	-67.1
	24-07-99	30	4000-8500	35	-67.4
	03-07-99	30	4000-8500	30	-68.1
CS 22497-34	15-07-99	30	4000-8500	35	-44.2
	24-07-99	30	4000-8500	40	-44.5
	03-07-99	30	4000-8500	35	-44.7

presented, and in Sect. 5 they are discussed and compared to other analyses of C-enriched stars. Finally, the concluding remarks are given in Sect. 6.

2. Observations

New high-resolution spectra were obtained for CS 22948-27 and CS 29497-34, in the blue region, using the 3.6m telescope at ESO, equipped with the Cassegrain Échelle Spectrograph (CASPEC). The log of observations is reported in Table 1. The wavelength range of the spectra is 3800–5000 Å, but they are only useful redward of 4000 Å because the flux was too faint at shorter wavelengths. A slit width of 250 μm was used, yielding a spectral resolving power (as verified from the measured widths of lines in the thorium comparison lamp) of $R = 21000$. For the previously obtained EMMI spectra the resolving power was $R = 30000$. The signal-to-noise ratio of the spectra has been estimated from the ADU level, as compared to stars with well-defined continua, at 4500 Å for the CASPEC data and at 6000 Å for the EMMI data; the resulting S/N values are reported in Table 1. Reductions were carried out using the packages developed by Spite (1990).

Because only $B - V$ colours were previously available for these stars (a measured colour for CS 22948-27, and an approximate colour for CS 29497-34), and the temperature is not accurately determined from this colour alone, new photometry of these stars in Johnson-Cousins B , V , R and I bands was obtained. The colours reported in Table 2 were derived using CCD observations obtained at the 0.9m Dutch telescope at ESO. The estimated calibration errors derived from the transformation

Table 2. Observed colours in Johnson-Cousins system (date of the observations: 09/09/1996)

Star	$V - B - V$	$V - R$	$V - I$	$R - I$
CS 22948-27	1.12	0.50	0.90	0.40
CS 29497-34	1.10	0.48	0.90	0.42
σ	± 0.016	± 0.015	± 0.016	± 0.005

from instrumental magnitudes to those in the standard system, using Landolt (1983, 1992) standards, are also given in Table 2. Because only one set of observations was obtained for each star, we are unable to comment on photometric errors arising from photon statistics, but these are expected to be small.

We draw attention to the fact that the measured colours are quite unusual: $B - V$ is larger than $V - I$, which is not expected in normal red stars. This is due to the fact that the atmospheres of these very metal-poor and C,N-enhanced stars are strongly affected by the presence of CH, CN and C_2 bands, producing huge gaps in the flux distribution of the stars. It is therefore mandatory to take these effects into account when deducing the temperature (Sec. 3.3). The reddening estimates toward these stars, obtained from the Burstein & Heiles (1982) maps, is minimal: $E_{B-V} = 0.00$ in the case of CS 22948-27, and $E_{B-V} = 0.01$ in the case of CS 29497-34, hence no adjustment to the measured colors has been made.

We have also obtained new high-resolution spectra with FEROS, at the 1.52m ESO telescope, for which radial velocities were measured in order to check for possible temporal variations (Table 1).

3. Calculations

Local Thermodynamic Equilibrium was assumed for the spectrum synthesis calculations. The code we employed for spectrum synthesis has been improved over the past thirty years, and has been described in Spite (1967), Barbuy (1982) and Cayrel et al. (1991). Solar abundances for the various elemental species were adopted from Grevesse et al. (1996). Oscillator strengths (gf values) for atomic lines were adopted from Wiese et al. (1969), Fuhr et al. (1988) and Martin et al. (1988) whenever available, otherwise they were obtained by fits to the solar spectrum.

The heavy neutron-capture elements lines and corresponding gf values given by Sneden et al. (1996) were added to our list of solar-identified lines. Hyperfine structure (HFS) corrections were taken into account for the elements Eu and Ba (Steffen 1985; François 1996). In the case of barium, the HFS correction is a delicate problem since this element has odd isotopes (mainly produced by r -process and having broad HFS) and even isotopes (produced by s -process and showing no HFS). The adopted HFS correction therefore depends on the s/r fraction assumed to have contributed to the enrichment of the star. On the other hand, Sneden et al. (1996) have shown that this issue is only important for the $\lambda 4554$ Å and $\lambda 4934$ Å lines, and unimportant for the three other lines $\lambda 5854$, $\lambda 6142$, and $\lambda 6497$ Å. Therefore, for the two bluest lines, we used the HFS structure

Table 3. Predicted colours and bolometric corrections computed from the MARCS99 CN-enhanced models.

T_{eff}	$\log g$	BC_K	BC_V	$B - V$	$V - R$	$V - I$	$R - I$	$V - K$	$J - H$	$J - K$	$K - L$
(1) $[C/H]=[N/H]=-1.0$ $[Fe/H]=-3.0$ dex											
4250	0.00	2.371	-0.693	1.611	0.707	1.356	0.649	3.064	0.656	0.794	0.122
	0.50	2.359	-0.618	1.580	0.656	1.267	0.612	2.977	0.657	0.803	0.129
	1.00	2.349	-0.561	1.567	0.617	1.200	0.584	2.910	0.652	0.809	0.135
	1.50	2.340	-0.520	1.575	0.591	1.154	0.563	2.860	0.642	0.812	0.143
4500	0.50	2.209	-0.478	1.329	0.605	1.183	0.578	2.687	0.607	0.716	0.086
	1.00	2.201	-0.437	1.319	0.575	1.127	0.553	2.638	0.607	0.723	0.090
	1.50	2.194	-0.404	1.327	0.552	1.084	0.533	2.598	0.602	0.726	0.095
	2.00	2.186	-0.379	1.352	0.537	1.054	0.518	2.565	0.590	0.725	0.102
4750	1.50	2.039	-0.325	1.066	0.508	1.022	0.516	2.364	0.561	0.650	0.066
	2.00	2.036	-0.308	1.090	0.498	1.000	0.503	2.344	0.556	0.652	0.069
	2.50	2.032	-0.288	1.123	0.491	0.983	0.493	2.320	0.543	0.648	0.075
5000	2.00	1.880	-0.255	0.857	0.450	0.929	0.480	2.135	0.515	0.584	0.054
	2.50	1.878	-0.249	0.886	0.447	0.922	0.475	2.127	0.511	0.585	0.056
	3.00	1.875	-0.238	0.925	0.447	0.916	0.470	2.113	0.499	0.581	0.061
(2) $[C/H]=[N/H]=+0.0$ $[Fe/H]=-2.0$ dex											
4750	2.00	1.999	-0.236	1.211	0.418	0.861	0.444	2.235	0.456	0.659	0.216
	2.50	2.000	-0.244	1.240	0.421	0.868	0.448	2.244	0.452	0.665	0.221
5000	2.00	1.861	-0.156	1.117	0.398	0.790	0.393	2.017	0.415	0.587	0.170
	2.50	1.861	-0.165	1.146	0.398	0.794	0.396	2.026	0.414	0.592	0.177
	3.00	1.862	-0.173	1.179	0.401	0.801	0.400	2.035	0.411	0.596	0.182
5250	2.50	1.724	-0.109	1.039	0.382	0.738	0.356	1.833	0.379	0.524	0.137
	3.00	1.724	-0.117	1.073	0.383	0.741	0.358	1.841	0.377	0.529	0.143
	3.50	1.725	-0.123	1.110	0.386	0.746	0.361	1.848	0.375	0.533	0.148

given by François (1996) (an adaptation of the original Rutten 1978) assuming a solar s/r mixture, and no HFS for the three reddest lines. Following Sneden et al. (1996), should the solar s/r mixture hypothesis be false and the enrichment be purely r -process, one would expect to have *overestimated* the Ba abundance from these two lines by at most 0.2 dex. The fact that we *do not* find any systematic difference between the blue and red Ba lines is a good indicator that the adopted hypothesis is acceptable.

3.1. Molecular lines

Absorption lines of the following molecules were taken into account in the calculations: MgH ($A^2\Pi-X^2\Sigma$), C_2 ($A^3\Pi-X^3\Pi$), CN blue ($B^2\Sigma-X^2\Sigma$), CH ($A^2\Delta-X^2\Pi$), CH ($B^2\Delta-X^2\Pi$), CN red ($A^2\Pi-X^2\Sigma$), TiO α ($C^3\Delta-X^3\Delta$), and TiO γ ($A^3\Phi-X^3\Delta$). ^{13}CH lines were also included, where wavelengths by Kurucz (1993) were corrected following Norris et al. (1997b) and Bonifacio et al. (1998).

In all cases where possible, the Franck-Condon factors with dependence on the rotational quantum number J , as given in Dwiwedi et al. (1978) and Bell et al. (1979), were computed and adopted. For vibrational bands where such values were not available, we adopted a constant value kindly provided to us through computations by Singh (1998, private communication).

For the blue CH and CN systems, the line lists by Kurucz (1993) were adopted, where we transformed his tables to our format, recomputing for each line the Hönl-London factors using the formulae by Kovacs (1979), revised according to Sharp

(1983). For the C_2 lines we have carried out a detailed comparison between the Kurucz (1993) line list and the laboratory list by Phillips & Davis (1968). The resulting molecular bands are very similar, thus we have kept the laboratory line list in most of our calculations.

We have adopted the electronic oscillator strengths $f_{\text{el}}(\text{CN red}) = 6.76\text{E-}3$ (Larsson et al. 1983; Davis et al. 1986; Bauschlicher et al. 1988) and $f_{\text{el}}(\text{CN blue}) = 0.0338$ (Duric et al. 1978), $f_{\text{el}}(C_2) = 0.033$ (Kirby et al. 1979), $f_{\text{el}}(\text{CH}) = 5.257\text{E-}3$ for the CH ($A^2\Delta-X^2\Pi$) (Brzozowski et al. 1976) and $2.5\text{E-}3$ for the CH ($B^2\Delta-X^2\Pi$) (Lambert 1978) and dissociation potentials $D_0(\text{CN}) = 7.65$ eV, $D_0(C_2) = 6.21$ eV, $D_0(\text{CH}) = 3.46$ eV (Huber & Herzberg 1979).

3.2. Model atmospheres

A special grid of plane-parallel model atmosphere was computed, hereafter referred to as MARCS99, using a revised version of the models described in Plez et al. (1992), taking into account the large enhancement of carbon and nitrogen in the atmosphere. These models are preliminary calculations, part of a new grid of Uppsala models based on an extensive update of the MARCS code (originally described by Gustafsson et al. 1975) and its input data. The grid ($4250 < T_{\text{eff}} < 5250$ K, $0.0 < \log g < 3.0$, $[Fe/H] = -3.0, -2.0$ and $[C/Fe] = +2.0$, $[N/Fe] = +2.0$) was especially adapted to represent these stars. The predicted colours for this grid of models were also calculated (Table 3), following Bessell et al. (1998), and used in the determination of the temperatures of our stars (Table 4).

Table 4. Stellar parameters: effective temperatures, surface gravities, metallicities, and microturbulence velocities v_t . In the upper part of the table, the temperatures deduced by a comparison of the observed and predicted colours are given, assuming two different chemical compositions: (1) $[C/H] = [N/H] = -1.0$, $[Fe/H] = -3.0$, (2) $[C/H] = [N/H] = 0.0$, $[Fe/H] = -2.0$

	CS22948-27		CS29497-34	
Assuming	(1)	(2)	(1)	(2)
T_{eff} from:				
$B - V$	4720	4990	4740	5030
$V - I$	5080	4620	5080	4620
$V - R$	4730	~4000	4830	~4150
$R - I$	~5500	4960	~5400	4860
Adopted parameters:				
T_{eff} (K)	4800		4800	
$\log g$	1.80		1.80	
$[FeI/H]$	-2.47		-2.90	
$[FeII/H]$	-2.46		-2.91	
v_t (km s $^{-1}$)	1.50		1.50	

3.3. Atmospheric parameter determination:

$$T_{\text{eff}}, \log g, [Fe/H], v_t$$

The colours of such metal-poor and C,N-enhanced stars are strongly affected by the presence of CH, CN and C₂ bands, producing large gaps in the stellar flux distribution. It is therefore mandatory to take these effects into account when deducing the temperature.

To determine the effective temperatures, we used the observed colours (Table 2), and compared them with the computed colours of the C,N-enhanced models (Table 3, assuming $\log g = 2.0$). In Table 4, these deduced temperatures are given assuming two different chemical composition for the models: ($[C/H] = [N/H] = -1.0$, $[Fe/H] = -3.0$) and ($[C/H] = [N/H] = 0.0$, $[Fe/H] = -2.0$). The dependence of temperature on the assumed C and N content is striking, emphasizing the need to use proper colour-temperature calibrations for C,N-enhanced stars. We note that the use of “normal” (i.e., non C,N-enhanced) colour calibrations would have led to a discrepancy in inferred temperatures for our stars as obtained from $B - V$ and $V - I$ of more than 700 K!

We have found that a temperature $T_{\text{eff}} = 4800$ K is the optimal choice for both stars. The measured H α profiles from our spectra are compatible with $T_{\text{eff}} \leq 4800$ K, which, when combined with photometric temperatures of Table 3, makes this a best choice. This temperature is also compatible with the excitation equilibrium of the Fe I lines and with the relative intensities of the (0,0) (1,1) and (1,0) (2,1) and (3,2) bandheads of C₂.

The same Fe I and Fe II line list (given in Paper I) was then used to determine the surface gravity $\log g$ (via ionization equilibrium) and v_t (via the requirement that estimated abundances are independent of the strength of the lines). The iron lines in the newly obtained blue spectra were not used for this purpose because of very severe blends with molecular lines.

The resulting atmospheric parameters are given in Table 4.

Table 5. Proper motions (given in mas)

Object	$\mu_{\alpha} \cos \delta$	error on $\mu_{\alpha} \cos \delta$	μ_{δ}	error on μ_{δ}	source
CS 22948-27	-2.0	6.3	-31.0	6.3	STN
CS 22948-27	0.1	2.2	-32.7	2.1	SPM
CS 29497-34	7.0	6.2	-29.0	6.2	STN
CS 29497-34	18.2	2.5	-27.1	2.3	SPM

3.4. Constraints from proper motions

Comparisons with the recent STARNET (STN; Fuchs 1999, private communication) and the Yale/San Juan Southern Proper Motion (SPM) 2.0 catalogs (Platais et al. 1998) has indicated that both of our program stars have measured proper motions. The data are presented in Table 5.

In both catalogs, the proper motions in declination are substantially larger than the corresponding errors. The SPM catalog proper motion in the right ascension component is also clearly much larger than the reported error. This has an important consequence on the maximum distances of our two stars, as it would be unreasonable to assume that our objects have total velocities greater than the escape velocity of the Galaxy. We now check if our choice of atmospheric parameters ($T_{\text{eff}} = 4800$ K, $\log g = 1.8$) is acceptable in this respect. From the following relationship:

$$\log \frac{g_*}{g_{\odot}} = \log \frac{M_*}{M_{\odot}} + 2 \log \frac{R_{\odot}}{R}$$

and assuming $M_* = 0.7 M_{\odot}$, one obtains

$$2 \log \frac{R_{\odot}}{R_*} = -2.49$$

and from:

$$0.4(M_{bol,*} - M_{bol,\odot}) = -4 \log \frac{T_{eff,*}}{T_{eff,\odot}} + 2 \log \frac{R_{\odot}}{R_*}$$

$M_{bol,*}$ is easily derived, assuming $M_{bol,\odot} = 4.75$ in conformity with the recommendations of the IAU (Andersen 1999).

The resulting value is:

$$M_{bol,*} = -0.67$$

Adopting the calculated MARCS99 bolometric correction appropriate to the effective temperature of 4800 K (Table 3) yields:

$$M_V = -0.35$$

and a distance modulus, $V - M_v$, of $12.65 - (-0.35) = 13.0$ (≈ 4 kpc) for CS 22948-27 and $12.20 - (-0.35) = 12.55$ (≈ 3.2 kpc) for CS 29497-34. Here we have assumed that the two stars are of identical luminosity and we neglect any interstellar absorption, as is appropriate for these high Galactic latitude objects.

Combining the estimated distances with the measured proper motions to obtain transverse velocities, and using our measured radial velocities, we obtain the U, V, W velocities

Table 6. Deduced spatial velocities (km s^{-1})

Name	U_{LSR}	V_{rot}	W_{LSR}
CS 22948-27	13	-367	66
CS 29497-34	1	-275	34

given in Table 6. We have adopted the convention that U is pointing towards the Galactic center, V towards the Galactic rotation direction, and W towards the north Galactic pole. We adopt the basic solar motion of Delhaye (1965; $U_{sun} = 9 \text{ km s}^{-1}$, $V_{sun} = 12 \text{ km s}^{-1}$, $W_{sun} = 7 \text{ km s}^{-1}$), and the relation between V_{rot} and V_{LSR} is $V_{rot} = V_{LSR} - 220 \text{ km s}^{-1}$. The total space velocities obtained are, respectively, 373 km s^{-1} and 277 km s^{-1} , well below the escape velocity corresponding to their location in the Galaxy, assuming a gravitational potential with constant rotational velocity.

Note that if we had adopted a significantly lower temperature, this would have induced a lower estimate of the surface gravity for our stars. A surface gravity of $\log g = 1.2$, for example, would make these two stars unbound to the Galaxy. Many of the carbon-enhanced stars found in the HK survey have significant proper motions, making it improbable that they are “normal” AGB stars of high luminosity, a hypothesis which might have otherwise been invoked to account for the very large carbon abundances via the classical third dredge-up scenario (though such a hypothesis would also have difficulty given that these stars are expected to be quite old based on their observed metallicities).

Both of our stars exhibit clear retrograde orbits in the Galaxy. The U , V , W components of their velocities are rather similar (small changes in their distance estimates could make them even more similar). This commonality of orbital motion for two stars which are so widely separated on the sky (and of similarly low metal abundance) *could* be due to chance, but it is intriguing to consider the possibility that they share a common origin, having been born in the same star forming region. Clearly, larger samples of such interesting stars are necessary to further explore this question.

4. Derived abundances

4.1. Molecular bands versus model atmospheres

In Fig. 1a we compare the partial pressures across the atmosphere, for CH, CN and C_2 using model atmospheres by Kurucz (1992), Gustafsson et al. (1975 and 1980, hereafter MARCS75) and the present models. Fig. 1b shows the reciprocal temperature as a function of the gas pressure, which traces the depth in the atmosphere.

The molecular concentration in the upper layers of the atmosphere is always lower in MARCS75 models due to a higher temperature, whereas in the Kurucz and Plez models, temperature tends to decrease towards the outer layers (Fig. 1b). As a consequence, the very strong lines, especially the molecular bandheads, are stronger in the Kurucz and MARCS99 models than in MARCS75 models.

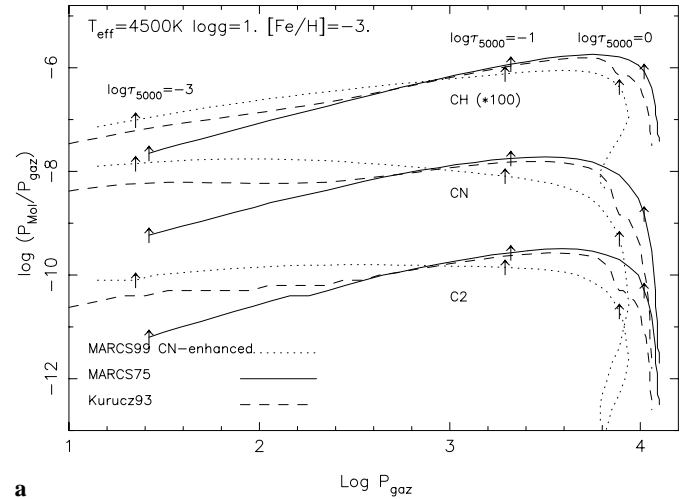
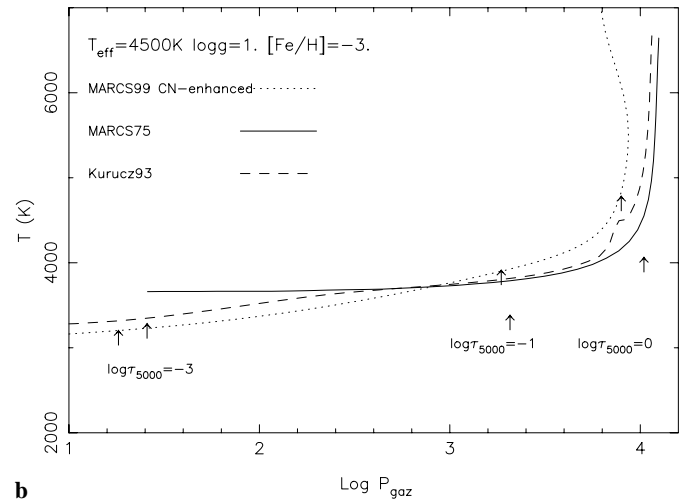
**a****b**

Fig. 1. **a** Log scale variation of the partial pressure of molecules (P_{mol}/P_{gas}) versus the gas pressure in three model atmospheres: MARCS99 (C, N enriched, *dotted lines*), MARCS75 (*solid lines*) and Kurucz (1993, *dashed lines*). The models were calculated for $T_{eff}=4500 \text{ K}$, $\log g=1.0$ and $[Fe/H]=-3.0$, and the dissociation equilibrium was calculated for $[C/Fe]=+2$. and $[N/Fe]=+2$. (The CH partial pressure was artificially multiplied by a factor 100 for the sake of clarity.) **b** Temperature variation versus the gas pressure for the same three models.

On the other hand, intermediate and weak lines forming at $\log(\tau) \simeq -1.0$ will be weaker with the MARCS99 models than with MARCS75 and Kurucz’s models, since the former is systematically hotter in the inner layers (Fig. 1b). The difference will be particularly evident for CN and C_2 , but less so for CH.

The shape of the computed molecular bands (from low to high vibrational transitions) will thus be very different when computed using a model atmosphere which explicitly takes into account the C and N overabundances or not (MARCS75, Kurucz). These changes are a result of the large differences in the temperature gradients inside the model stellar atmospheres. Deep in the atmosphere, the pressure inversion in the MARCS99 models is due to turbulent pressure in the convection zone.

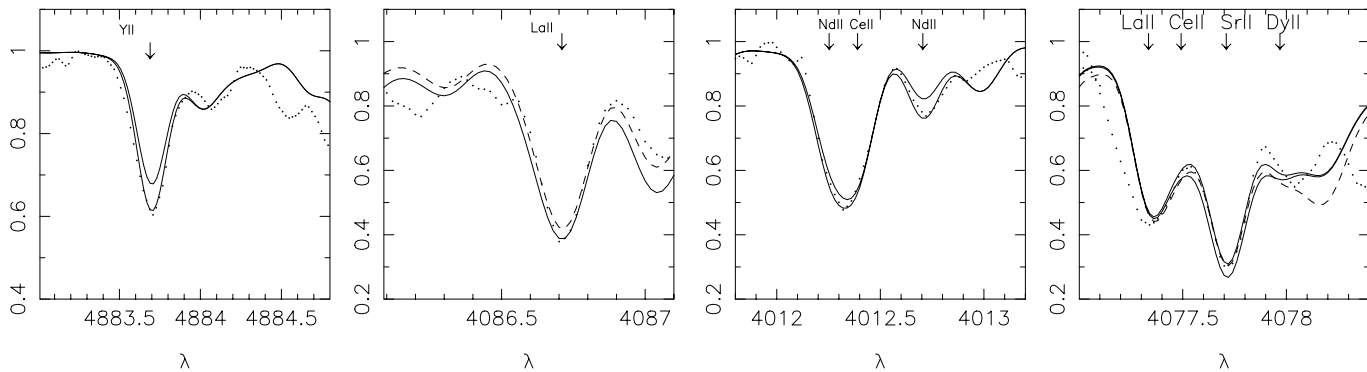


Fig. 2. CS 22948-27: Y II 4883.69 and La II 4086.68 Å lines computed with respectively $[Y/Fe] = +0.8, +1.2$ dex and $[La/Fe] = +2.5, +2.7$ dex. The observed spectrum is displayed as dots. In the right panel, the dashed lines show the effect of increasing the C abundance by 0.2 dex, showing that the blending CN line introduces an uncertainty of ~ 0.3 dex on the derived La abundance.

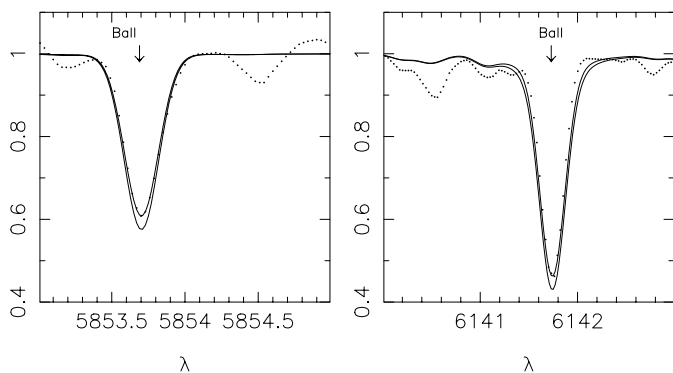


Fig. 3. CS 29497-34: Ba II $\lambda 5853.69$ and $\lambda 6141.73$ Å lines computed with $[Ba/Fe] = +1.9, +2.1$.

4.1.1. Results given by different models

In Paper I we used classical MARCS75 models to represent these C-rich stars. It is clear from the discussion above that one should use appropriate models when possible. Using standard models in this case may introduce discrepancies between the strong and weak features of a single molecule, and also discrepancies between features of different molecules. For example, it might be expected that the abundance deduced from C_2 lines and CH lines (which are stronger) will disagree: the C_2 lines will be overestimated (leading to low C abundances) and the CH features will be underestimated (leading to high C abundances).

However, comparing the synthetic spectra calculated with the present models with the observed spectra of our stars, we found that the C_2 bands did not have exactly the right shape: the very strongest lines (the bandheads themselves) are slightly overestimated with respect to the medium to weak lines. This is most probably due to the fact that the models do not represent very well the atmosphere in the outermost layers, which could be due to the neglect of opacities from carbon-bearing polyatomic molecules. Therefore, in our analysis, we discarded the

Fig. 4. CS 29497-34: Nd II $\lambda 4012.03$ and Sr II $\lambda 4077.7$ Å lines computed with, respectively, $[Nd/Fe] = +1.8, +2.1$ and $[Sr/Fe] = +1.0, +1.2$ (solid lines). The observed spectrum is displayed as dots. In the right panel, the dashed line shows the effect of increasing the C abundance by 0.2 dex.

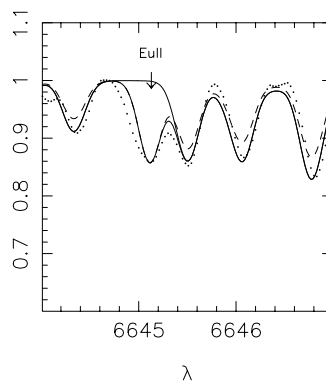


Fig. 5. CS 22948-27: Eu II $\lambda 6645.13$ Å computed for $[Eu/Fe] = 0.0$ and $+2.1$ (solid lines). The dashed line corresponds to a change in the intensity of CN bands, obtained by decreasing the C abundance by 0.2 dex.

very strongest lines and relied on lines of moderate strength to determine the C and N abundances.

Some disagreement appears with our previous measurements (Paper I, where we used MARCS75 models), as well as between CH and C_2 bands for carbon. The C abundances derived from C_2 lines are about 0.5 dex higher than those derived from the CH G band (Table 8). This is possibly due to problems in the line lists, in addition to the model atmosphere problem outlined above – the same discrepancy has been found by Bonifacio et al. (1998). The most probable values of the C abundance are summarized in Table 8.

4.2. Heavy neutron-capture elements ($Z > 35$)

In view of the discrepancies pointed out in Sect. 4.1 concerning the intensity of CH versus C_2 lines, we adjusted the C and N abundances around each atomic line of interest.

Owing to the severe blending (mostly by molecular bands) effects on many of the atomic lines, the abundances of the neutron-capture elements were all determined by synthetic spectrum fitting. Figs. 2 to 5 show the typical fits obtained, and also

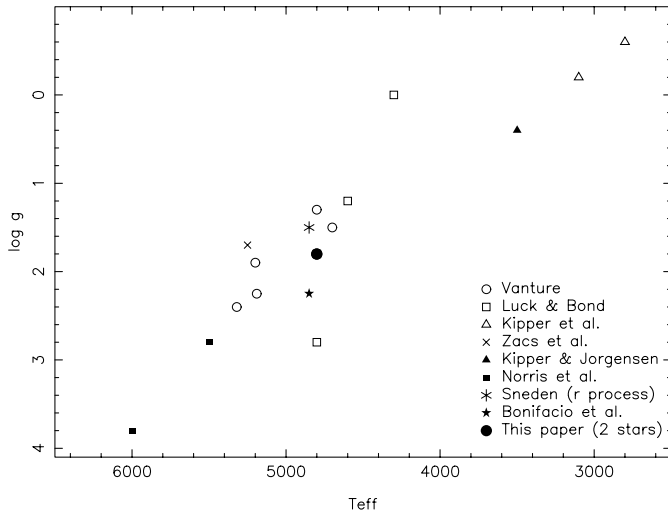


Fig. 6. $\log g$ vs. T_{eff} for metal-poor carbon-rich stars, with data points by Vanture (1992), Luck & Bond (1991), Kipper et al. (1996), Kipper & Jørgensen (1994), Norris et al. (1997a), Sneden et al. (1996), Bonifacio et al. (1998), Zacs et al. (1998) and our present stars.

indicate the effect of uncertainties on the C and N abundances. The line-by-line abundances are summarized in Table 7, where we report results only for the lines that were not too severely blended by strong molecular bands. In this table, a (:) sign denotes a very uncertain abundance, which was then *not used* to compute the mean abundance of the element reported in Table 8. Also reported in Table 8 are the $1\text{-}\sigma$ dispersion of the abundances derived from all the lines of a given element (when three or more lines could be measured). The abundance patterns of the heavy elements as a function of atomic number are illustrated in Fig. 7.

The Th II $\lambda 4019.13 \text{ \AA}$ line which has been observed in CS 22892-52 (interestingly, another C-enhanced star) has been discussed at length by many other authors (Sneden et al. 1996; Norris et al. 1997b; Cowan et al. 1999). The interest in the derivation of an accurate Th abundance is clear, since this radioactive element can serve as a chronometer to measure the age of a star (provided suitable comparison r -process elements are also observed). Unfortunately, at the resolution of our spectra this is not possible because there is a strong ^{13}CH line falling on top of it (as was cautioned by Norris et al. 1997b). For the two stars under study here, although an absorption line is clearly visible at $\lambda 4019.13 \text{ \AA}$, the uncertainty on the carbon abundance and $^{12}\text{C}/^{13}\text{C}$ ratio does not allow us to determine the real thorium contribution to the blend. We therefore prefer not to make use of this chronometer based on the present data.

Europium is a very critical element to measure since it is thought to be produced almost solely by the r process. The main lines of this element are Eu II $\lambda 4129.7$, $\lambda 4205.05$, $\lambda 6437.64$ and $\lambda 6645.13 \text{ \AA}$. Unfortunately, both the $\lambda 4129.7$ and $\lambda 4205.05 \text{ \AA}$ lines are too severely blended by CN lines to determine abundances from them. The lines measured were thus the two reddest ones. The Eu II $\lambda 6645.13 \text{ \AA}$ is illustrated in Fig. 5.

4.3. Lithium abundance

The Li I $\lambda 6707 \text{ \AA}$ line was also measured in both CS 22948-27 and CS 29497-34, and the derived lithium abundances are given in Table 8. Both stars exhibit lithium abundances which are *lower* than the estimated primordial abundance, as expected for giant stars, which are capable of diluting their initial lithium by internal mixing processes. The rather low $^{12}\text{C}/^{13}\text{C}$ ratio found in these stars (14 and 12 respectively for CS 22948-27 and CS 29497-27, derived from the CN lines at $\lambda\lambda 8003\text{--}8004 \text{ \AA}$ – see Paper I), is similar to the ratio found in typical field halo giants (Sneden et al. 1986, Pilachowski et al. 1997¹), and in these stars, such a low value is interpreted as due to mixing. On the other hand, the observed Li abundance might be considered “high”, since lithium is not often detected in metal-poor giants. This high Li abundance is an argument in favor of an additional supply of Li by mass transfer from an evolved companion (AGB) providing both Li and s - elements. Other metal-poor C-rich stars are known in the literature with various Li abundances (e.g., Norris et al. 1997a) – the dwarfs and subgiants having seemingly larger Li abundances than the giants, in agreement with the effect of mixing in giants. Variations on these ideas could be considered, such as a common envelope evolution.

5. Discussion of the abundances

In Fig. 6 we compare, in the form of a $\log g$ vs. T_{eff} diagram, the derived atmospheric parameters for our program stars with those of other metal-deficient C-rich stars discussed in the recent literature. The open symbols represent mildly metal-deficient C-rich stars, in the abundance range $-2.0 < [\text{Fe}/\text{H}] < -1.0$; the filled symbols represent very metal-poor C-rich stars with $[\text{Fe}/\text{H}] < -2.5$. Metal-poor carbon stars are found in a large region of the HR diagram, from main-sequence turnoff stars ($\log g \approx 3$) to the very evolved cool giants ($\log g < 0$). The interpretation of the phenomenon depends in particular on the evolutionary stage of the star. Most of these stars are rich in heavy elements from Sr to Sm. However, in the case of one star, CS 22957-27 (Norris et al. 1997b; Bonifacio et al. 1998), these elements have been found to be underabundant relative to iron.

A variety of elemental abundance distributions among the heavy elements are exhibited in metal-poor stars. For example, in the so-called CH stars, where the s -process elements are enhanced, the ratio of the heavy s elements to the light s elements (the $[\text{hs}/\text{ls}]$ ratio in the definition of Luck & Bond 1991) is larger than in the sun – $[\text{hs}/\text{ls}]$ is positive and may exceed 1.0 dex (Vanture 1992). In the very metal-poor star CS 22892-52 (Sneden et al. 1996), the heavy elements are enhanced, but the ratio $[\text{hs}/\text{ls}]$ is only around 0.4 dex, because the enhancement is due to the r -process. Also, owing to the large abundance of Eu (a nearly pure r -process element), $[\text{Ba}/\text{Eu}]$ is nearly as low as -1.0 dex. The

¹ Let us note that in this paper, CS 22948-27 and CS 29497-34 are both quoted and appear in their Fig. 3 with the $\log g$ value from our Paper I. Our current work provides significantly larger values of $\log g$ for these two stars that would then lie much closer to the mean distribution

Table 7. Line-by-line elemental abundances. $\epsilon(X)$ is the logarithmic value = $\log(X/H) + 12$.

	λ	χ	$\log gf$	CS 22948-27		CS 29497-34	
				[X/Fe]	$\epsilon(X)$	[X/Fe]	$\epsilon(X)$
NaI	5889.97	0.00	0.117	0.44:	4.30:	1.12	4.55
NaI	5895.94	0.00	-0.184	0.69:	4.55:	1.47	4.90
MgI	5172.70	2.71	-0.380	0.39	5.5	0.62	5.3
SrII	4077.71	0.00	0.17	0.90	1.34	1.00	1.00
YII	4883.70	1.08	0.07	1.20	0.98	1.20	0.54
YII	5087.43	1.08	-0.17	0.80	0.58	1.00	0.34
YII	5123.22	0.32	-0.93	1.00:	0.78:	0.80:	0.14:
YII	5200.42	0.99	-0.57	0.70:	0.48:	0.80:	0.14:
BaII	4554.03	0.00	0.17	2.30	1.97	2.10	1.33
BaII	4934.10	0.00	-0.15	2.10	1.77	2.00	1.23
BaII	5853.69	0.60	-1.01	2.30	1.97	1.90	1.13
BaII	6141.73	0.70	-0.07	2.30	1.97	1.90	1.13
BaII	6496.91	0.60	-0.38	2.30	1.97	2.25	1.48
LaII	4042.91	0.93	0.32	2.40:	1.16:	2.30:	0.62:
LaII	4077.33	0.23	-0.16	2.70:	2.46:	3.10:	1.42:
LaII	4086.71	0.00	-0.16	2.70	1.46	2.30	0.62
LaII	5123.01	0.32	-0.93	1.95:	0.71:	1.95:	0.27:
LaII	6320.43	0.17	-1.52	1.95	0.71	1.95	0.27
CeII	4042.59	0.50	0.10	0.70:	-0.21:	-	-
CeII	4077.49	0.30	-0.38	1.50:	0.59:	1.70:	0.35:
CeII	4222.60	0.12	-0.18	2.20	1.29	2.00	0.65
CeII	4562.37	0.48	0.33	-	-	1.90	0.55
PrII	5220.12	0.80	0.17	1.65	-0.10	1.65	-0.54
PrII	5259.74	0.63	-0.07	2.60:	0.85:	-	-
NdII	4012.25	0.63	0.60	2.40	1.44	2.10	0.70
NdII	4023.01	1.00	0.38	2.70	1.74	2.50	1.10
NdII	4059.96	0.20	-0.60	2.60:	1.64:	-	-
NdII	4061.09	0.47	0.30	3.80:	2.84:	3.00:	1.60:
NdII	5212.35	0.20	-0.70	2.40	1.44	2.20	0.80
NdII	5234.21	0.55	-0.46	2.60	1.64	2.20	0.80
NdII	5249.60	0.98	0.08	1.85	0.89	1.85	0.45
NdII	5293.17	0.82	-0.20	1.85	0.89	2.00	0.60
NdII	5311.48	0.99	-0.56	2.40	1.44	-	-
NdII	5319.82	0.55	-0.35	1.85	0.89	1.85	0.45
NdII	5361.51	0.68	-0.40	1.85	0.89	2.00	0.60
NdII	5442.29	0.68	-0.90	1.95	0.99	-	-
SmII	4023.23	0.04	-0.83	1.70:	0.24:	2.00:	0.10:
SmII	4042.90	0.10	-0.36	2.40:	0.94:	2.30:	0.40:
EuII	6437.64	1.32	-0.28	2.10	0.15	2.25	-0.14
EuII	6645.13	1.38	0.20	2.10	0.15	2.25	-0.14
DyII	4077.96	0.10	-0.05	1.50:	0.14:	1.50:	-0.30:
DyII	5169.69	0.10	-1.66	1.60	0.24	1.50	-0.30

two very metal-poor stars (a main sequence turn-off star and a subgiant star) recently observed by Norris et al. (1997a) exhibit elemental patterns suggesting an s -process production of the heavy elements. The [hs/lr] ratio in these two stars is as high as 1.5 dex, and [Ba/Eu] is around 0.7 dex, in clear contrast with the star CS 22892-52. The most likely interpretation, as suggested by the authors, is the accretion of matter from an AGB (a phase producing both carbon and s elements) companion.

In Fig. 7 we present a detailed comparison of the abundance patterns of several heavy elements in our two program stars with other C-enriched stars, in particular, the metal-poor C-

Table 8. Mean abundances for Li, C, Na, Mg and heavy elements

element	CS	22948-27	CS	29497-34		
$\epsilon(\text{Li})$	+0.3		+0.1			
$^{12}\text{C}/^{13}\text{C}$	14		12			
	[X/Fe]	σ	N	[X/Fe]	σ	N Z
C(C ₂)	+2.05			+2.5		
C(CH) ^a	+1.9			+2.35		
C(CH) ^b	+1.5			+1.9		
N(CN)	+1.8			+2.3		
Na	>0.56	-	2	+1.30	-	2 11
Mg	+0.39	-	1	+0.62	-	1 12
Sr	0.90	-	1	1.00	-	1 38
Y	1.00	0.28	2	1.10	0.14	2 39
Ba	2.26	0.09	5	2.03	0.15	5 56
La	2.32	0.53	2	2.12	0.25	2 57
Ce	2.20	-	1	1.95	0.07	2 58
Pr	1.65	-	2	1.65	-	1 59
Nd	2.22	0.35	11	2.09	0.21	8 60
Eu	2.10	-	2	2.25	-	2 63
Dy	1.60	-	1	1.50	-	1 66

^a from moderate strength lines around 4000 Å

^b from the G band (very strong lines)

rich stars analysed by Kipper & Jørgensen (1994), Kipper et al. (1996), Norris et al. (1997a), and the very-metal-poor r -process enriched star CS 22892-52 (Sneden et al. 1996; Cowan et al. 1995; Norris et al. 1997b). For clarity, we have restricted the comparison to the elements also present in our results.

The heavy-element abundance patterns of these C-rich stars exhibit a variety of characteristics. The behaviour of the metal-poor carbon stars, illustrated by that of HD 25408 (Kipper et al. 1996), compared to ours (Fig. 7b), shows that the abundance ratios between the heavy elements (in particular [hs/lr]) are quite different from our program stars. One case closer to ours is that of HD 187216 (Kipper & Jørgensen 1994), where unfortunately Eu and Dy were not measured. Note that HD 189711 (Kipper et al. 1996) exhibits a similar pattern as observed in our two program stars and has an overall heavy element overabundance of the same order (whereas HD 187216 has an even larger enhancement of these heavy species). The abundance pattern of our stars is also rather similar to the stars LP 625-44 and LP 706-7 (Norris et al. 1997a) shown in Figs. 7e,f. Finally, a comparison with CS 22892-52 (Fig. 7a) indicates how different this “ r -process star” is from all the others.

In Fig. 8 we show the expected pattern of r -process and s -process enrichment, as described by Norris et al. (1997a), where our abundances are overplotted in Figs. 8a,b, compared to the same plot for CS 22892-52 and LP 625-44 (Fig. 8c,d). It is known (Sneden et al. 1996; Norris et al. 1997b) that the abundances of CS 22892-52 are well fit by a scaled solar r -process pattern (see however Gorieli & Arnould 1997).

We see that the abundance patterns of our two stars lie roughly half-way between these two predicted nucleosynthesis scenarios, at least for the heavier elemental species. The same

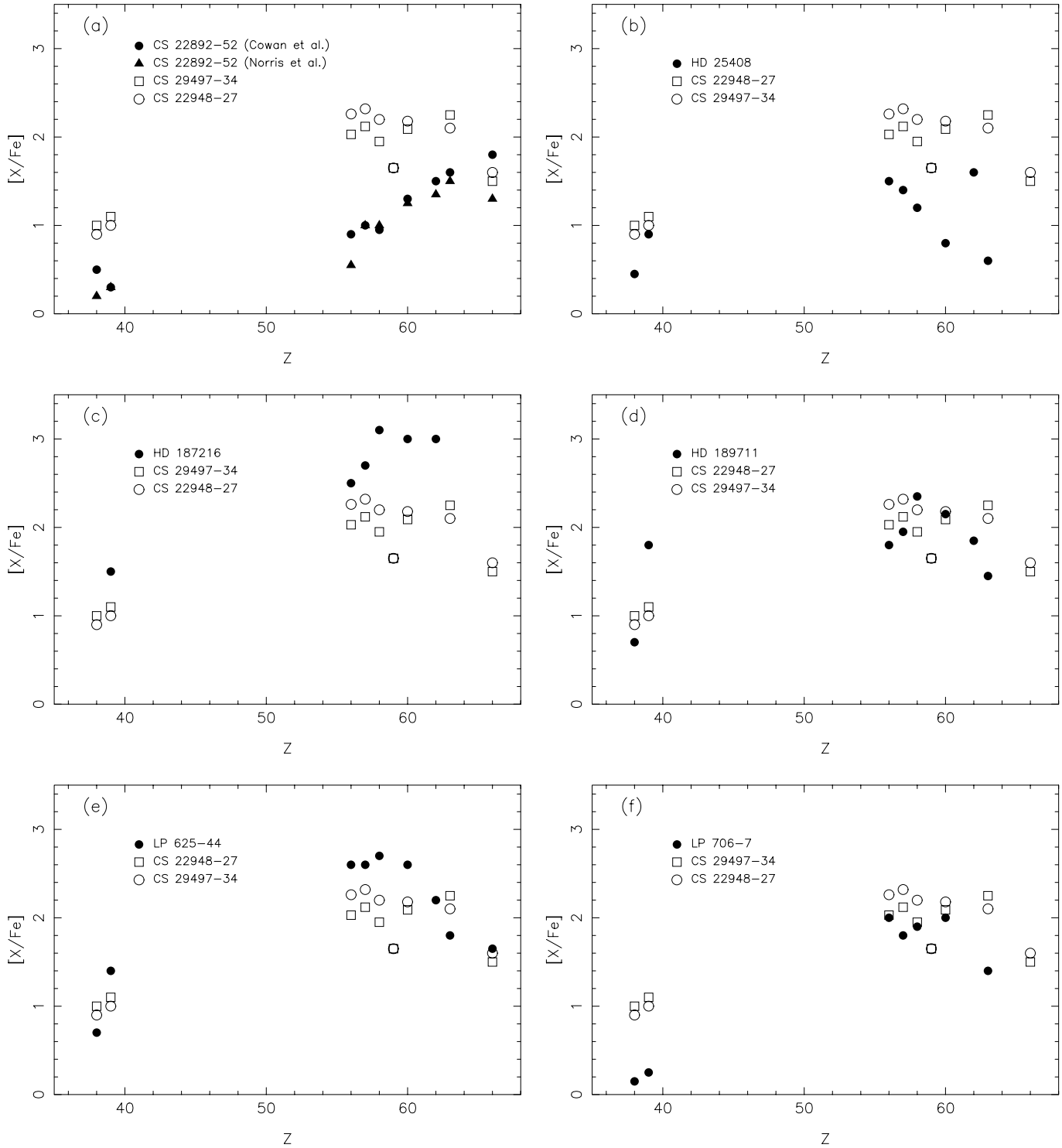


Fig. 7a–f. $[X/Fe]$ abundance ratios for neutron-capture elements ($Z > 35$), versus the Atomic Number Z .

conclusion is reached regarding the $[Ba/Eu]$ and $[hs/ls]$ abundance ratios as given in Table 9 – our stars show ratios intermediate between those of CS 22892-52 and the s -element stars LP 625-44 and LP 706-7. Kipper & Jørgensen’s star HD 187216 is also rather well fit by an r -process (although Eu is missing in their determinations).

5.1. Interpretation

At first inspection, the huge carbon enhancements found in CS 22948-27 and CS 29497-34 suggest a scenario, originally proposed by Iben (1982), which induces a very efficient production of carbon in zero-metal (Population III stars) of moderate mass. The carbon may even be violently mixed (Fujimoto et

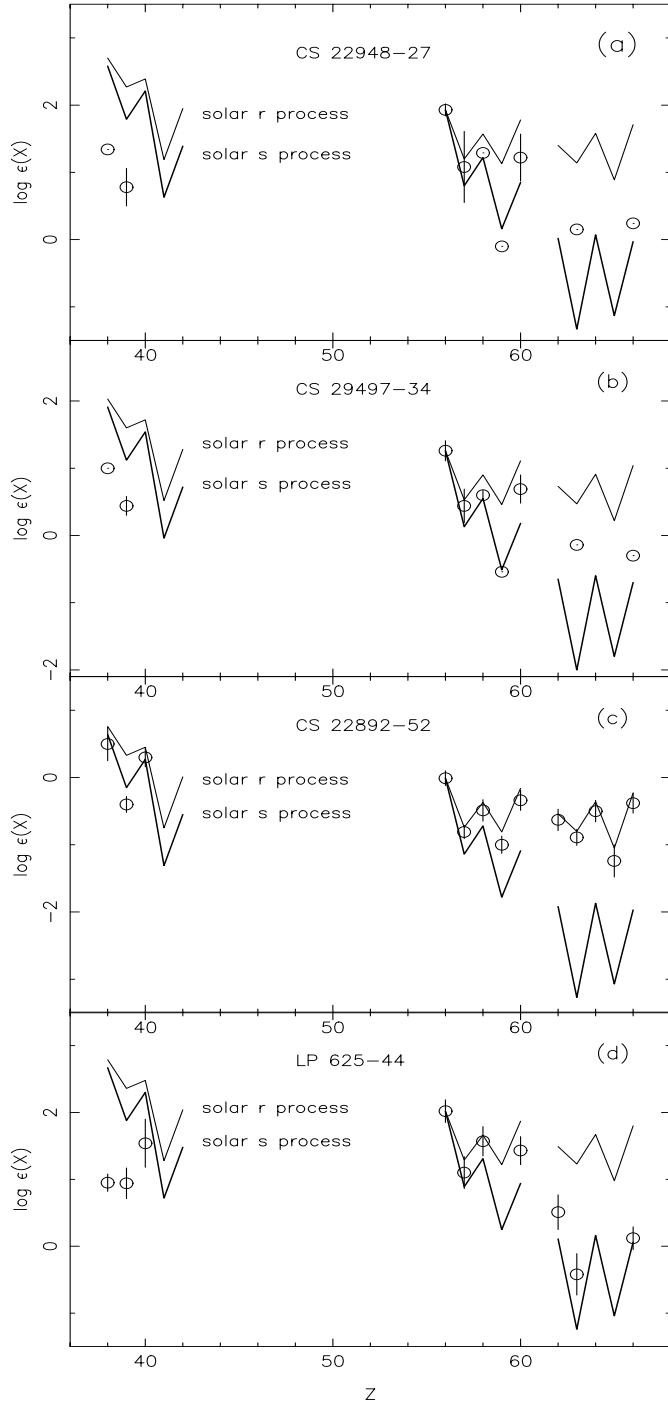


Fig. 8a–d. Observed abundance pattern of the neutron-capture elements compared to the solar *s*- (thick line) and *r*-process (thin line) patterns, normalized to Ba ($Z = 56$), as in Sneden et al. (1996). The standard deviations were computed (see Table 8) when more than one line was measured, and the error bars are indicated accordingly.

al. 1990, 1999; Hollowell et al. 1990), also producing large amounts of nitrogen, and bringing these elements to the stellar surface. This scenario, however, would predict a $^{12}\text{C}/^{13}\text{C}$ ratio near the equilibrium value, whereas our measurements provide a significantly larger value. In addition, the luminosity of

Table 9. $[\text{Ba}/\text{Eu}]$ and $[\text{hs}/\text{ls}]$ computed as in Norris et al. (1997a): $[\langle \text{Ba}, \text{Ce}, \text{Nd} \rangle] / [\langle \text{Sr}, \text{Y}, \text{Zr} \rangle]$

star	$[\text{Ba}/\text{Eu}]$	$[\text{hs}/\text{ls}]$
LP 625-44	0.82	1.39
LP 706-7	0.61	1.76 to 1.44
CS 22948-27	0.06	1.26
CS 29497-34	-0.06	0.97
CS 22892-52	-0.85 (-0.67 to -0.97)	0.5
Sun	0.00	0.00
HD 122563	-0.50	-0.50 to 0.00

a post-He-core flash star, even in this exceptional scenario, is expected to be rather high. Also, the presence of metals has to be explained. Fujimoto et al. (1995) propose accretion from interstellar clouds as one possible process, but any stellar wind during the lifetime of these stars would make this accretion rather inefficient. Moreover, the high observed Eu/Fe ratio would restrict the accretion specifically to those clouds which themselves possess high Eu/Fe ratios – a very improbable process.

Another plausible scenario would be mass transfer from an evolved companion. A Population II binary of low metallicity may have evolved to the point that the (present-day) secondary star has accreted the mass ejected by its companion in the AGB phase, and we observe now the low mass secondary, enriched in C, N and *s*-elements. Some Pop. II stars are known with a relatively high Eu/Fe ratio. Norris et al. (1997a) also suggest such a transfer scenario for their two stars, which are rather similar to ours (see Figs. 7 and 8). They also find that one of their stars has indeed a variable velocity, suggesting binarity. To check this interpretation we have carefully measured the radial velocity in all the available spectra of our stars. Let us note that in our Paper I there was a mistake in the computation of the heliocentric corrections, and thus all the radial velocities of the red spectra should be replaced by the ones in Table 1. In the red (EMMI spectra for $\lambda > 5000 \text{ \AA}$), we estimate that the radial velocity precision is about 1.5 km s^{-1} (the blending of lines in these spectra makes it difficult to obtain more accurate radial velocities at our resolution). In the blue spectra, the radial velocities were estimated from the position of the hydrogen lines (mainly $\text{H}\beta$) and the uncertainty is larger, of the order of 3 km s^{-1} . From the resulting values given in Table 1, we see that there is no clear evidence of binarity from the radial velocities. One of the Norris et al. (1997a) stars, LP 625-44, which exhibits a rather similar abundance pattern to both of our program stars, has been shown by Ryan (1999, private communication), on the basis of recent high-resolution data, to exhibit a definite binary signature in its radial velocity data, and a period of more than 2000 days. Further long term followup of CS 22948-27, CS 29497-34, and others like them, preferably with higher resolution spectroscopy, should be carried out. Let us recall that in Sect. 4.3, we noted that the “intermediate” lithium abundance is compatible with both a strong dilution of the primordial abundance by convective dilution (as observed in Pop II giants), compensated by an enhancement caused by the transfer of Li-rich mass from the

companion. Let us also recall that the “intermediate” value of the $^{12}\text{C}/^{13}\text{C}$ ratio is similar to the intermediate value observed by Aoki & Tsuji (1997) in metal-poor CH stars (mostly known to be binaries). These authors interpret this value by some compensation between mass transfer (bringing additional ^{12}C) and convective mixing (decreasing the $^{12}\text{C}/^{13}\text{C}$ ratio). The lithium and carbon isotopes observed in our two stars are therefore compatible with the mass transfer scenario.

Another possible interpretation would be the evolution of a single low mass Pop. II star (with Eu already present from some previous enrichment of the ISM) through the AGB phase and the third dredge-up. This is, however, a rather short lived episode in a stellar lifetime, and it would be remarkable to have found two such similar stars in this same evolutionary stage at the same time. Furthermore, a rather high luminosity is then expected, in contradiction with the rather large values of surface gravity derived for our stars (and supported by the observed proper motions).

Finally, it is important to note that the amount of enrichment in C, N and in the heavy elements (relative to iron) for our program stars is among the highest found up to now.

6. Conclusions

We have carried out a revised analysis and derivation of heavy-element ($Z > 35$) abundances in the very metal-poor CH/CN-strong stars CS 22948-27 and CS 29497-34, originally discovered as part of the ongoing HK survey. These stars show among the highest C and N enhancements relative to Fe known, which, in combination with their relatively low effective temperatures, results in very strong CH, C₂ and CN bands. The blending of lines, particularly in the blue, presents a great problem for abundance derivation from atomic lines based on observations with resolving power $R \sim 20000 - 30000$. Nevertheless, by making use of spectrum synthesis fitting, it has been possible to derive the abundances of the neutron-capture heavy elements Sr, Y, Ba, La, Ce, Pr, Nd, Eu, and Dy.

The abundance patterns of the neutron-capture elements in CS 22948-27 and CS 29497-34 appear to be intermediate between *s*-process and a *r*-process enrichment patterns. These stars would therefore be different from the well-known “*r*-process star” CS 22892-52 (Sneden et al. 1996). The *s*-process contribution might be well due to a mass-transfer episode from an evolved companion star. Our radial velocity measurements show no significant variations, i.e., no indications of binarity, but are not sufficiently accurate, nor do they extend over a sufficiently long temporal baseline to exclude this hypothesis either.

Our present observations of these two stars suggest that these giants are not Pop III stars, polluted either by internal or external processes, but rather, they are very metal-poor stars, enhanced in C, N and *s*-process elements (and Eu) either because the matter which formed these stars happened to be enriched in these elements, or by mass transfer from an evolved companion. It is somewhat surprising that the two stars we have analyzed are so similar, even though they are separated by about 30° in

the sky, but of course no firm conclusions can be derived from such a small sample.

The full understanding of these very metal-poor and C,N-rich stars, revealed to be numerous in the HK survey, clearly warrants detailed investigation through the analysis of a much larger sample.

Acknowledgements. We are indebted to T. Augusteijn and S. Ortolani for the observation and reduction of photometric data. We are also grateful to P. D. Singh for the calculation of Franck-Condon factors of the blue systems of CH and CN, to B. Castilho for calculations of molecular intensity factors, and to B. Fuchs for making available the STN proper motion measurements of our stars. We also thank P. Bonifacio for his very useful remarks as a Referee of the paper. We acknowledge partial financial support from the Observatory of Paris, CNPq/CNRS and Fapesp. BN acknowledges financial support by the Carlsberg Foundation. TCB acknowledges financial support by the National Science Foundation (US), through grant AST 95-29454. BP thanks S. Johansson and the Atomic spectroscopy division of Lund University for their hospitality. This work made use of the Simbad database at CDS, Strasbourg.

References

- Andersen J., 1999, Transactions of the IAU Vol. XXIII B, Kluwer Acad. Pub., Dordrecht (Holland)
- Aoki W., Tsuji T., 1997, A&A 317, 845
- Barbuy B., 1982, PhD thesis, Univ. Paris VII
- Barbuy B., Cayrel R., Spite M., et al., 1997, A&A 317, L63
- Bauschlicher C.W., Langhoff S.R., Taylor P.R., 1988, ApJ 332, 531
- Beers T.C., Preston G.W., Shectman S.A., 1985, AJ 90, 2089
- Beers T.C., Preston G.W., Shectman S.A., 1992, AJ 103, 1987
- Bell R.A., Dwiwedi P.H., Branch D., Huffaker J.N., 1979, ApJS 41, 593
- Bessell M.S., Castelli F., Plez B., 1998, A&A 333, 221 (erratum A&A 337, 321)
- Bonifacio P., Molaro P., Beers T.C., Vladilo G., 1998, A&A 332, 672
- Brzozowski J., Bunker P., Elander N., Erman P., 1976, ApJ 207, 414
- Burstein D., Heiles C., 1982, AJ, 87, 1165
- Cayrel R., Perrin M.-N., Barbuy B., Buser R., 1991, A&A 247, 108
- Cowan J.J., Burris D.L., Sneden C., McWilliam A., Preston G.W., 1995, ApJ 439, L51
- Cowan J.J., Pfeiffer B., Kratz K.L., et al., 1999, in press (astro-ph/9808272)
- Davis S.P., Shortenhaus D., Stark G., et al., 1986, ApJ 303, 892
- Delhaye J., 1965 in: Galactic Structure vol. 5 of the Compendium “Stars and Stellar systems” by Kuiper and Middlehurst, University of Chicago Press 1965.
- Duric N., Erman P., Larson M., 1978, Phys. Scripta 18, 39
- Dwiwedi P.H., Branch D., Huffaker J.N., Bell R.A., 1978, ApJS 36, 573
- François P., 1996, A&A 313, 229
- Fuhr J.R., Martin G.A., Wiese W.L., 1988, *Atomic Transition Probabilities: Iron through Nickel*, Journal of Physical and Chemical Reference Data, vol. 17, suppl. no. 4
- Fujimoto M.Y., Iben I. Jr., Hollowell D., 1990, ApJ 349, 580
- Fujimoto, M.Y., Sugiyama, K., Iben, I. Jr., Hollowell, D. 1995, ApJ 444, 175
- Fujimoto, M.Y., Aikawa, M., Iben, I. Jr. 1999, in 3rd Stromlo Symposium: The Galactic Halo, ASP Conf. Ser. 666, 247
- Goriely, S., Arnould, M. 1997, A&A 322, L29

- Grevesse, N., Noels, A., Sauval, J.: 1996, in ASP Conf. Ser. 99, eds. S.S. Holt, G. Sonneborn, p. 117
- Gustafsson, B., Bell, R.A., Eriksson, K., Nordlund Å., 1975, A&A 42, 407
- Gustafsson, B., Bell, R.A., Fredga, K., Gahm, G.F., 1980, A&A 89, 225
- Hollowell, D., Iben, I. Jr., Fujimoto, M.Y. 1990, ApJ 351, 245
- Huber, K.P., Herzberg, G. 1979, *Constants of Diatomic Molecules*, van Nostrand Reinhold, New York
- Iben, I. Jr. 1982, ApJ 260, 821
- Kipper, T., Jørgensen, U.G. 1994, A&A 290, 148
- Kipper, T., Jørgensen, U.G., Klochkova, V.G., Panchuk, V.E. 1996, A&A 306, 489
- Kirby, K., Saxon, R.P., Liu, B. 1979, ApJ 231, 637
- Kovacs, I. 1979, *Rotational Structure in the Spectra of Diatomic Molecules*, Am. Elsevier Pub. Co.
- Kurucz, R. 1992, in IAU Symp. 149, eds. B. Barbuy & A. Renzini, Kluwer Acad. Press, p. 225
- Kurucz, R. 1993, CD-ROM 18
- Lambert D.L., 1978, MNRAS 182, 249
- Landolt, A.U. 1983, AJ 88, 439
- Landolt, A.U. 1992, AJ 104, 340
- Larsson, M., Siegbahn, P.E.M., Ågren, H. 1983, ApJ 272, 368
- Luck R. E., Bond, H. 1991, ApJS 77, 515
- McClure, R.D., Fletcher, J.M., Nemeč, J.M. 1980, ApJ 238, L35
- McClure, R.D., Woodsworth, W. 1990, ApJ 352, 709
- Martin, G.A., Fuhr, J.R., Wiese, W.L. 1988, *Atomic Transition Probabilities: Scandium through Manganese*, Journal of Physical and Chemical Reference Data, vol. 17, suppl. no. 3
- Norris, J.E., Ryan, S.G., Beers, T.C. 1997a, ApJ 488, 350
- Norris, J.E., Ryan, S.G., Beers, T.C. 1997b, ApJ 489, L169
- Phillips, J.G., Davis, S.P. 1968, *The Swan System of the C₂ molecule*, Univ. of California Press
- Pilachowski, C., Sneden, C., Hinkle, K., Joyce, R. 1997, AJ 114, 819
- Platais, I., Girard, T.M., Kozhurina-Platais, V., et al., 1998, AJ, 116, 2556 (SPM)
- Plez, B., Brett, J.M., Nordlund, Å. 1992, A&A 256, 551
- Rossi, S., Beers, T.C., Sneden, C. 1999, in 3rd Stromlo Symposium: The Galactic Halo, ASP Conf. Ser. 666, 268
- Rutten R.J., 1978, Sol. Phys. 56, 237
- Sharp, C. 1983, PhD thesis, Univ. of St. Andrews
- Sneden, C., Pilachowski, C. A., VandenBerg, D. A. 1986, ApJ 311, 826
- Sneden, C., McWilliam, A., Preston, G.W., et al., 1996, ApJ 467, 819
- Spite, M. 1967, Ann. Astrophys. 30, 211
- Spite, M. 1990, ESO Data analysis workshop, ESO Conf. and Workshop Proceedings N.34, eds. D. Baade and P. Grosbøl, p. 125
- Steffen M. 1985 A&AS 59, 403
- Vanture A. D. 1992, AJ 104, 1997
- Wiese, W.L., Martin, G.A., Fuhr, J.R. 1969, *Atomic Transition Probabilities: Sodium through Calcium*, NSRDS-NBS 22
- Začs, L., Nissen, P.E., Schuster, W.J. 1998, A&A 337, 216